

Volume 2, Number 2, pp. 68-86, 2000.

◀ Home Current Issue Table of Contents ►

Computer Modelling of the Sinoatrial Node

H. Zhang*, A.V. Holden* and M.R. Boyett

* School of Biomedical Sciences, University of Leeds, Leeds, United Kingdom

Correspondence: henggui@cbiol.leeds.ac.uk

Abstract. Mathematical models are used to investigate the ionic basis underlying the pacemaking activity of central and peripheral SA node cells. Differences in the intrinsic electrophysiological properties are responsible for the regional differences in their electrical activities. Such regional differences underlie the mechanism of dynamic behaviours of the intact SA node, such as pacemaker shift.

Keywords: Sinoatrial node, pacemaker, ionic currents, pacemaker shift, propagation

Introduction

The sinoatrial node (SA node) is the pacemaker of the heart. It initiates rhythmical action potentials in the heart. Mathematical models have been produced of the electrical activity of the SA node [7, 9, 24, 31]. These models are of a typical SA node action potential, and ignore the heterogeneities of the SA node in functions, anatomy and electrophysiology [2, 3, 6, 8, 12, 16, 20, 25, 28, 29, which are essential for modelling accurately the initiation and propagation of the action potentials in the heart. Models incorporating the regional differences within the SA node activity have been developed [24, 32]. These models were based on speculation, because of the absence of data at the time on regional differences in ionic currents. Recently, based on experimental data of the kinetics of ionic channels, the ionic current densities and their regional differences, models of action potentials for central and peripheral SA node cells have been developed [35]. The model action potentials have the same characteristics and regional differences as those recorded experimentally [12]. Here we used the newly developed models [35] to investigate the ionic basis underlying the spontaneous activity of SA node cells, and their regional differences. We also studied the integrated behaviours of an intact SA node model, which incorporates the regional differences in the electrophysiological properties of SA node [4, 12, 13, 16, 17, 18, 19, 22]. We show that gradient distributions in the ionic current densities of SA node cells are responsible for the regional differences in their electrical activities and responses to ionic channel blockers. Such differences underlie the dynamical behaviours of the intact SA node, such as the pacemaker shift in response to a variety of interventions [25].

Methods

Heterogeneity of the SA node

The SA node is a heterogeneous tissue. Cells in the centre are smaller and have fewer and more poorly organised myofilaments than cells in the periphery [2]. Electrical activities recorded from the intact SA node or small pieces of tissue have shown that in the centre, the take-off potential is more positive, the action potential upstroke velocity is slower, the action potential duration is longer, the maximum diastolic potential (also resting potential in quiescent tissue) is more positive, and pacemaking rate is paradoxically slower than in the periphery [16, 18, 25]. In normal circumstance, the action potential is first initiated in a small part of the SA node, called the leading pacemaker site, which is approximately in the centre of the SA node. Once initiated, the action propagates towards the periphery and then the atrial muscle. The propagation is asymmetric. The action potentials propagate preferentially towards the upper crista terminalis direction, but is blocked in the block zone in the septum direction. The action potentials then encircle the SA node, and re-excite the SA node in the block zone [3]. The block zone is functionally important, because it protects the sinoatrial node from invasion by arrhythmias. The leading pacemaker site is dynamic. In response to a variety of interventions, for example autonomic nerve stimulation, the leading pacemaker site shifts from the centre and in many cases it shifts towards the periphery [25]. (see movie 1(Spread of depolarisation from the sinoatrial node (mpeg file); movie 2 (Spread of action potential (mpeg file))

Regional differences in current densities - experiments vs. model

The electrical activity varies from the centre to the periphery of the intact SA node in a characteristic fashion [16]. Such a variation could be explained by a gradual decrease of the atrial modulation [5, 30, 33] from periphery to centre of SA node. However atrial modulation cannot explain the remarkable differences of electrical activities in small balls cut from different regions of SA node (in which the large mass of surrounding atrial muscle is removed) [16, 25]. There are two radically different interpretations to explain such regional differences. One is the MOSAIC model [29]. In the MOSAIC model, it has been conjectured that the electrophysiological properties of individual pacemaker cells in the node are uniform and the apparent regional differences in electrical activity in the intact SA node are the result of a progressive increase in the percentage of intermingling atrial cells towards the periphery giving rise to a progressive increase in their hyperpolarizing influence from centre towards the periphery. However, the MOSAIC model failed [34] to generate action potentials with the same regionally dependent characteristics as those seen experimentally [16, 25]. The other one is the gradient model [6]. In the gradient model, it is believed that the regional differences in the electrical activity are due to a gradient distribution of ionic current densities in cells from periphery to the centre of the SA node [6].

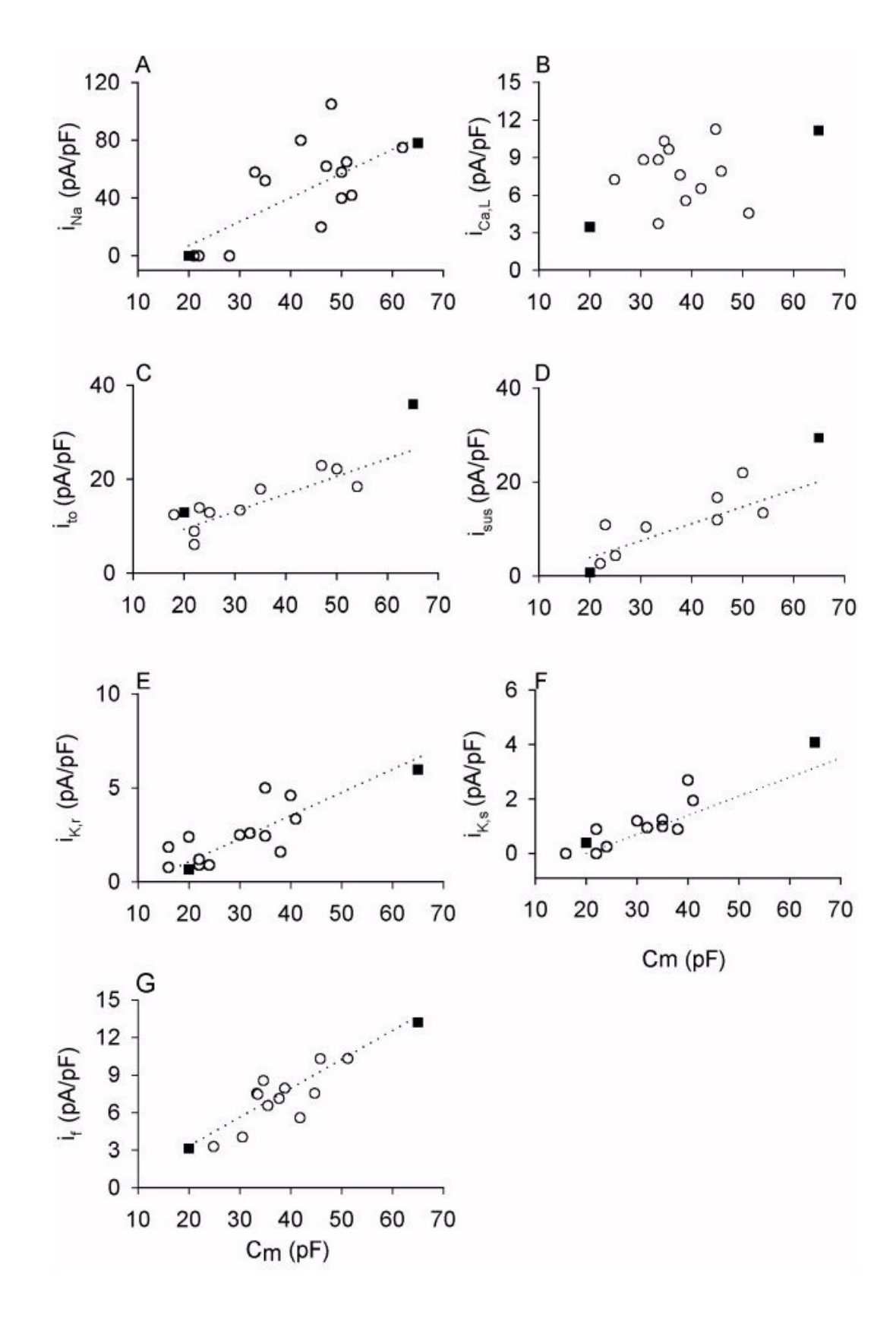


Figure 1. Correlation of ionic current density and cell capacitance. Ionic current densities are plotted against the cell capacitance for adult rabbit sinoatrial node cells. Open circles: experimental data. Solid squares: values computed from the models. In the models, we assume a cell capacitance of 20 pF for a central sinoatrial node cell; and of 65 pF for a peripheral sinoatrial node cell. (A) i_{Na} ; (B) $i_{Ca,L}$; (C) i_{to} ; (D) $i_{K,sus}$; (E) $i_{K,r}$; (F) $i_{K,s}$.

Figure 1 shows the densities of various currents plotted against the cell capacitance, a measure of cell size. Though single cells have not yet been isolated from the centre and periphery of the SA node, it has been found that the electrical activity of rabbit SA node cells is correlated with cell size, and small cells have properties characteristic of the centre of the SA node and large cells have properties characteristic of the periphery [12]. In the figure, the open symbols are the experimental data obtained from rabbit SA node cells [12, 13, 19]. Figure 1A shows the density of i_{Na} (measured during a 10 ms pulse to -5 mV from a holding potential of -60 mV), Fig. 1B shows the density of i_{Ca,L} (measured during a 300 ms pulse to 0 mV from a holding potential of -40 mV), Fig. 1C shows the density of i_{to} (measured during a 200 ms pulse to +50 mV from a holding potential of -60 mV), Fig. 1D shows the density of 4-AP-sensitive sustained current (measured during 200 ms pulse to +50 mV from a holding potential of -60 mV), Fig. 1E shows the density of i_{K,r} (measured as the peak tail current during a 1 s pulse to -10 mV from a holding potential of -50 mV), Fig. 1F shows the density of i_{K,s} (measured as the peak tail current during a 1 s pulse to +40 mV from a holding potential of -50 mV) and Fig. 1F shows the density of if (measured at the end of a 300 ms pulse to -110 mV from a holding potential of -40 mV). The densities measured experimentally of all currents are significantly correlated with cell capacitance and are larger in cells with a higher capacitance [12, 13, 19].

In Figure 1, filled squares are the computed densities of ionic currents for central (cell capacitance 20 pF) and peripheral (cell capacitance 65 pF) cells with the same protocol as used in experiments. Values for all the densities of the ionic currents for the peripheral and central SA node cell models are within the experimental range and are greater in the peripheral SA node cell model.

Peripheral and central SA node action potentials - experiments vs. model

Figure 2A, B shows the action potentials generated using the models at fast (Fig. 2A) and slow (Fig. 2B) time bases. For comparison, Fig. 2C, D shows action potentials recorded experimentally from rabbit SA node preparations. Figure 2C shows action potentials at a fast time base recorded from small balls of tissue from the periphery and centre of the SA node at a temperature of 32°C. Figure 2D shows action potentials at a slow time base recorded from single cells with capacitances of 22.5 and 55 pF at a temperature of 35°C. The simulated action potentials are similar to those recorded experimentally. The model peripheral action potential has a more negative take-off potential, a more rapid upstroke, a more positive peak value, a greater amplitude, a shorter duration and a more negative maximum diastolic potential than the model central action potential. Furthermore, the spontaneous activity of the peripheral cell model is faster than that of the central cell model. All of these are characteristic differences seen experimentally, either between small balls of tissue from the periphery and centre of the rabbit SA node [16] or large and small rabbit SA node cells [12] and can be seen in Fig. 2C, D. The action potential from the peripheral SA node model has an early rapid phase of repolarization (phase 1) after the action potential upstroke. Such an early rapid phase of repolarization after the action potential upstroke can be observed frequently in the periphery of the intact SA node (not in the centre) and in small balls of tissue from the periphery (not from the centre) [4, 22].

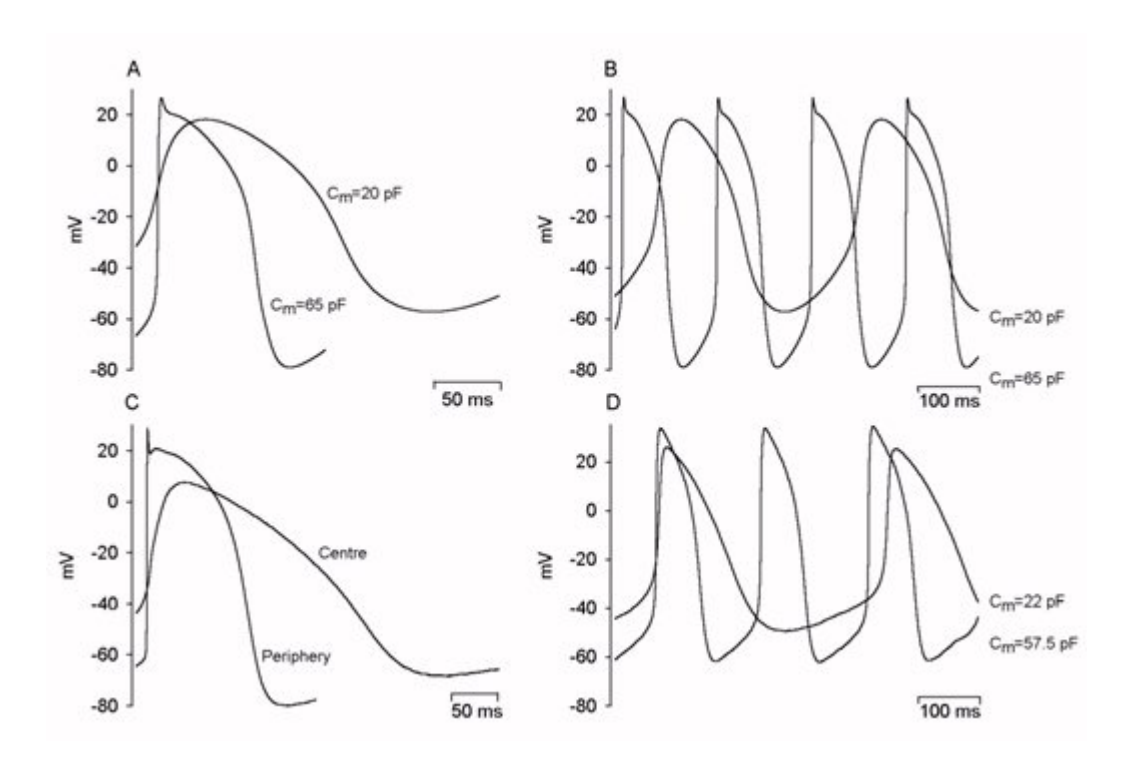


Figure 2. Simulated peripheral and central SA node action potentials. The action potentials of central and peripheral sinoatrial node cells. (A) generated by the models at a fast time base. (B) generated by the models at a slow time base. (C) recorded from small balls from centre and periphery of rabbit SAN at a fast time base. (D) recorded from single cells of rabbit SAN at a slow time base (from Zhang et al. [35]).

In Figure 3 we compare the characteristics of the simulated action potentials with the characteristics of action potentials recorded experimentally from a set of rabbit SA node cells from [12] at 35°C. In Fig. 3, the open circles show experimental data from [12] - the takeoff potential (TOP) (Fig. 3A), maximal upstroke velocity of the action potential (dV/dt) (Fig. 3B), action potential amplitude (Fig. 3C), action potential duration (Fig. 3D) (APD), maximal diastolic potential (MDP) (Fig. 3E) and cycle length (CL) (time between successive spontaneous action potentials; Fig. 3F) of single rabbit SA node cells are plotted against the cell capacitance, C_m. In all cases (except for action potential duration) there are significant correlations of the variables with C_m. In Fig. 3, the filled squares show corresponding values from the peripheral and central cell models. In all cases, the model values are close to those recorded experimentally; the changes with cell capacitance are also comparable to those seen experimentally. Although no correlation was observed experimentally between action potential duration and C_m in rabbit SA node cells, there was a difference in action potential duration in the peripheral and central cell models (Fig. 3D). However, the action potential duration in the peripheral and central cell models are still comparable to the data from rabbit SA node cells (Fig. 3D) and, furthermore, in small balls of tissue from the periphery and centre of the rabbit SA node a regional difference in action potential duration is observed [4] similar to that between the peripheral and central SA node cell models (Fig. 3D).

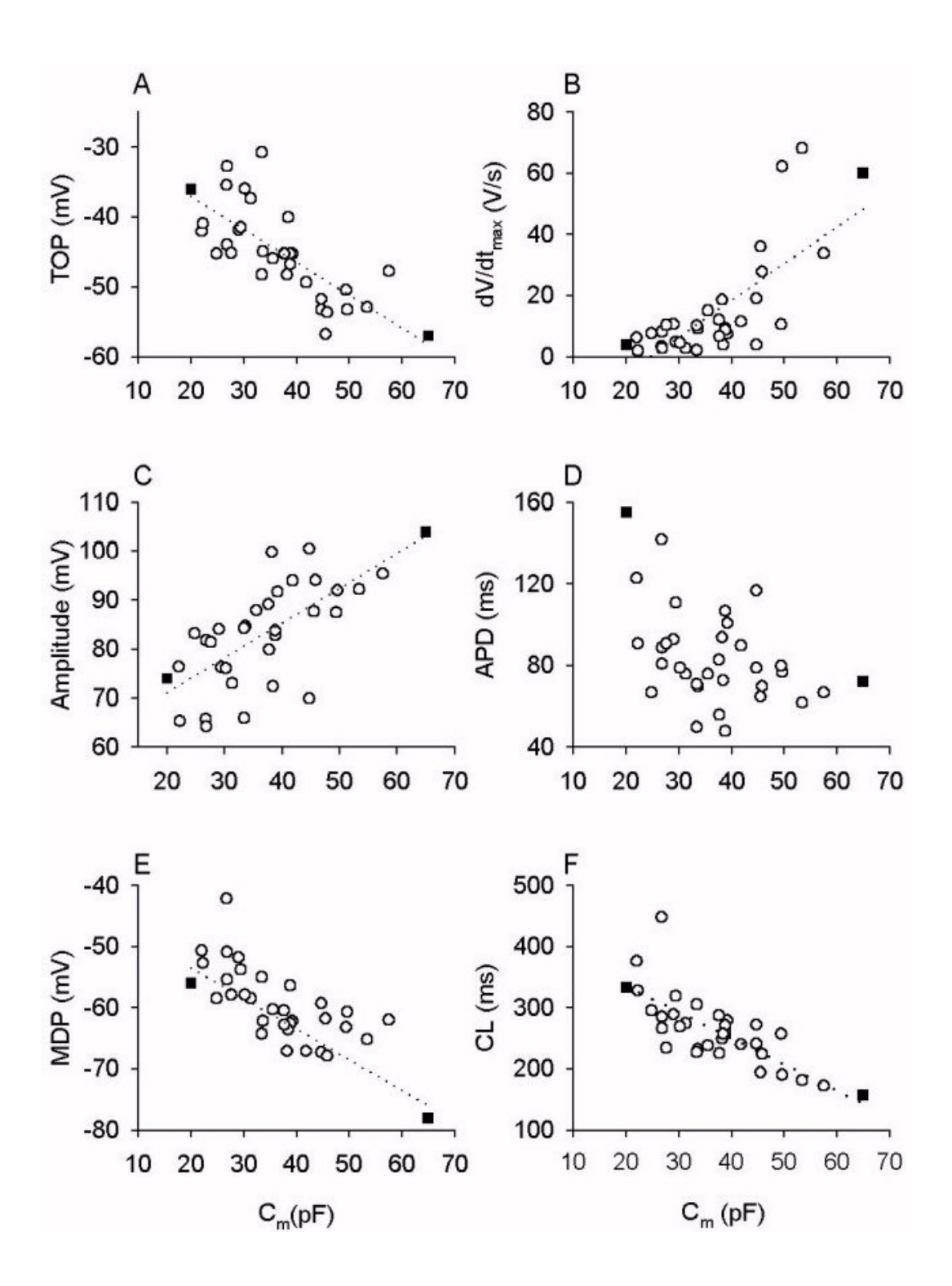


Figure 3. Correlation of action potential characteristics and cell capacitance. The comparison of the characteristics of action potentials of central and peripheral sinoatrial node cells between simulation and experiment. Open circle: data obtained from adult rabbit sinoatrial node cells; Solid square: values computed from models. Once again, in the model, we assume the cell capacitance of a central sinoatrial node cell is 20 pF, and a peripheral cell 65 pF. The values computed from models are consistent with those obtained experimentally. (A) take-off potential (TOP). (B) maximal upstroke velocity. (C) amplitude of action potential. (D) action potential duration (APD). (E) maximal diastolic potential (MDP). (F) spontaneous pacemaking cycle length (CL) (from Zhang et al. [35]).

Role of each ionic current in the pacemaker activity

The pacemaking activity of SA node cell is the cooperative effect of all individual ionic channel currents. To analyse the role of each individual current in the pacemaking activity, we look at the effect of blocking the current on the action potentials.

(a) Role of i_{Na} . Figure 4A shows the effect of block of i_{Na} on peripheral (left panel) and central (right panel) action potentials. Blocking i_{Na} had no effect on the central action potential. In contrast, blocking i_{Na} had various effects on the peripheral action potential: (i) the take-off potential was shifted to a more positive potential; (ii) the upstroke velocity of the action potential was dramatically reduced after block of i_{Na} from 60 to 8 V/s - after block of i_{Na} , the upstroke velocity in the periphery was approximately the same as that in the centre); and (iii) as a result of the change in the take-off potential, spontaneous activity was slowed after block of i_{Na} .

In the peripheral cell model, block of i_{Na} also reduced the peak value of the action potential, the action potential duration and the maximal diastolic potential; these changes are also seen experimentally in small balls of tissue from the periphery of the rabbit SA node tissue [18].

In conclusion, i_{Na} mainly contributes in the depolarisation phase and is responsible for a large upstroke velocity of action potentials. In the peripheral SA node tissue, unlike that in central SA node tissue, pacemaking is sensitive to block of i_{Na} .

(b) Role of $i_{Ca,L}$. Figure 4B shows the effect of block $i_{Ca,L}$ (simulation of Nifidipine) on peripheral (left) and central (right) action potentials. In simulation, block of $i_{Ca,L}$ abolished the action potential in the centre of the SA node: the membrane potential settled at -42 mV (this is very close to that seen experimentally, in which membrane potential settled at -45 mV [18]). In contrast, in the periphery block of $i_{Ca,L}$ had different effects on electrical activity. Block of $i_{Ca,L}$: (i) shortened the action potential; (ii) increased the pacemaking rate (presumably as a consequence of the shortening of the action potential); in the simulation, block of $i_{Ca,L}$ causes a 22.5 % increase in the pacemaking rate (similar to that seen in experiments, 2 M nifedipine caused a 21 ± 1 %, mean ± SEM, n=15, increase in the pacemaking rate [18]); (iii) decreased the maximal upstroke velocity and (v) decreased the overshoot of the action potential. In the simulation, block of $i_{Ca,L}$ caused a decrease of maximal upstroke velocity from 60 to 40 V/s and a decrease in the peak of the action potential from 27 to 8 mV (in experiments, on the application of 2 M Nifedipine, the maximal upstroke velocity was decreased from 82 to 75 V/s, and the peak of the action potential was decreased from 22 to 6 mV [18]).

In conclusion, pacemaking in the central SA node tissue, unlike that in peripheral SA node tissue, is sensitive to block of $i_{Ca,L}$.

- (c) Role of $i_{Ca,T}$. Figure 4C shows the effect of block of $i_{Ca,T}$ (simulation of Ni⁺). Hagiwara et al. (11) reported that block of $i_{Ca,T}$ by 40 mM Ni²⁺ produced on average a 14.4 % increase in the cycle length in rabbit SA node cells. In simulation, both the peripheral (left) and central (right) SA node cell models, block of $i_{Ca,T}$ caused a small increase in cycle length of 4 and 19 % respectively, similar to that reported experimentally [11]. In simulations, block of $i_{Ca,T}$ has very little effect on peripheral model action potential, but has different effects on central model action potential: (i) shortened the action potential duration; (ii) decreased the amplitude; (iii) increased the maximal diastolic potential.
- (d) Role of $i_{K,r}$ Figure 4D shows the effect of block of $i_{K,r}$ (simulation of E-4031) on peripheral and central action potentials. In simulation complete block of $i_{K,r}$ caused the cessation of spontaneous activity in peripheral and central tissue. After complete block of

 $i_{K,r}$, the membrane potential settled at -33 mV in the peripheral cell model, and -30.3 mV in the central cell model, this is similar to that seen experimentally (the membrane potential settled at -34.96±1.94 mV on average in rabbit peripheral SA node tissue, at -32.04±1.95 mV on average in rabbit central SA node tissue [17]). This shows that, in both the periphery and centre, $i_{K,r}$ is important for pacemaking. $i_{K,r}$ is responsible for generating the maximum diastolic potential, and thus when $i_{K,r}$ is blocked, the membrane during diastole is depolarised and spontaneous activity ceases.

Partial block of $i_{K,r}$ has different effects on the action potentials in peripheral and central rabbit SA node tissue. With $i_{K,r}$ blocked by 50%,it abolishes the action potentials in central tissue, but not in peripheral tissue. In the periphery cell model, partial block of $i_{K,r}$: (i) increase action potential duration; (ii) increases the cycle length; and (iii) decreases the maximal diastolic potential. This is similar to that seen experimentally [17]

(e) Role of 4-AP-sensitive current. Figure 4E shows the effect of block of 4-AP-sensitive current on peripheral (right) and central (left) action potentials. 4-AP blocks both transient and sustained outward current, i_{to} and $i_{K,sus}$. The effect of 4-AP was simulated by blocking both i_{to} and $i_{K,sus}$ (and 10% $i_{K,r}$). In the simulation, 4-AP caused (i) prolongation of the action potential in both peripheral and central cells. In simulations, 4-AP caused an increase of 50% in APD for the peripheral cell model, and 21% for the central cell model (experimentally 5 mM 4AP increased the APD by 66±4% for small ball from periphery, 25±5% for small ball from centre of rabbit SA node (13)); (ii) an increase in the action potential overshoot; (iii) an increase in the cycle length in the peripheral tissue and a decrease in cycle length in the central tissue. In the simulation, 4-AP caused about 3.0% decrease in the cycle length for the central cell model, about 26.5% increase in the cycle length for the peripheral cell model (experimentally, 5 M 4-AP caused an decrease of 4.5±2% in cycle length in small ball from centre, an increase of 28±6% of cycle length in small ball from periphery [13]).

It can be concluded that 4-AP-sensitive current plays a major role in action potential repolarization and its role varies regionally.

- (f) Role of $i_{K,s}$ Complete block of $i_{K,s}$ has very little effect on the pacemaker activity of both peripheral and central cell models.
- (g) Role of i_f . Figure 4F shows the effect of block of i_f (simulation of Cs⁺) on peripheral and central action potentials. Block of i_f slowed spontaneous activity and the slowing was greater in the periphery. In the simulations, block of i_f caused a 34 % increase in the cycle length in the peripheral cell model and a 7.6 % increase in the central cell model (in experiments, block of i_f caused on average a 25 % in peripheral tissue and a 7 % in central tissue [21, 22]). In the simulations at least, the greater effect of block of i_f on the peripheral SA node cell model can be explained by the greater density of i_f in the peripheral model.

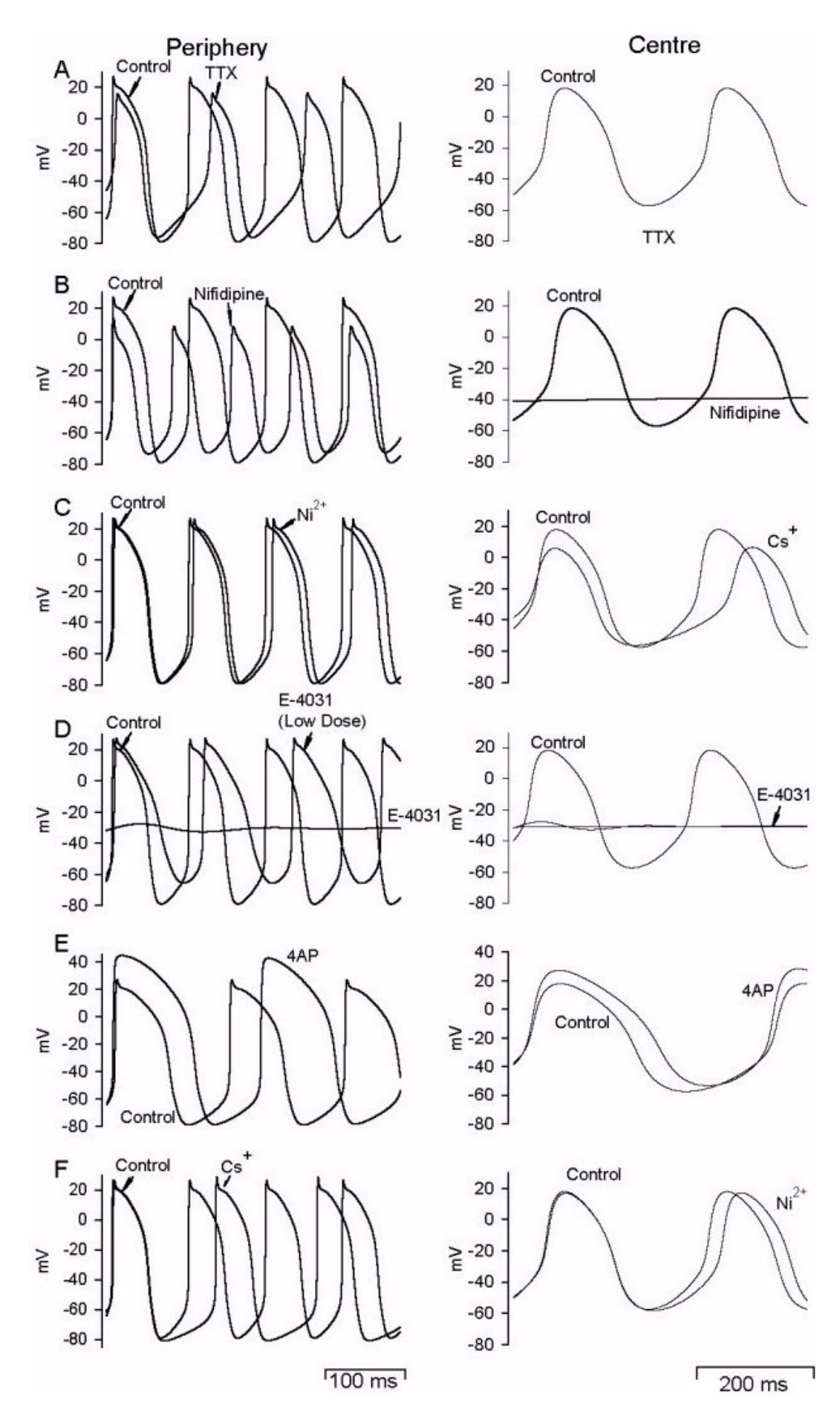


Figure 4. A. Effect of block of i_{Na} . Blocking i_{Na} has no effect on the pacemaker activity of the central SA node cell, but slows down the pacemaker activity of the peripheral SA

node cell. B. Effect of block of $i_{Ca,L}$. Blocking $i_{Ca,L}$ abolished the action potential for the central SA node, but in the peripheral SA node, the pacemaker activity maintains, with a faster rate, and a small action potential duration. C. Effect of block of $i_{Ca,T}$. Blocking $i_{Ca,T}$ slows down the pacemaker activity of SAN cells. D. Effect of block 4-AP-sensitive current. Blocking 4AP-sensitive current causes the prolongation of action potential durations for both central and peripheral sinoatrial node cells, increases the pacemaker activity rate in the centre, but slows down the pacemaker activity rate in the peripheral. E. Effect of block $i_{K,r}$. Blocking $i_{K,r}$ abolished the action potential for the central SA node, but in the peripheral sinoatrial node, the pacemaker activity maintains, with a slower rate, and a larger action potential duration. F. Effect of block of i_f . Blocking i_f slows down the pacemaker activity in both the central and the peripheral sinoatrial node. The effect in the peripheral is significant, while in the centre is small.

Model of Intact sinoatrial node

It is known that the functioning of the SA node is not only dependent on the properties of the cells making up the SA node - it is also dependent on the multicellular nature of the SA node and the electrotonic interaction between the SA node and the atrial muscle surrounding the SA node [15]. Based on the models developed for peripheral and central SA node cells [35], a one-dimensional partial differential equation of multicellular model for the SA node and atrium was developed. In the model, the multicellular SA node and atrium is modelled as a string of cells with a length L; of this the string of SA node cells has a length, L^S, of 3.0 mm (similar to the distance from the centre of the SA node to the atrial muscle in the rabbit heart [2]) and the string of atrial cells has a length, L^a, of 9.6 mm. Within the string of SA node cells, we assume that the capacitance changes from 20 (cell capacitance in central cell model) to 65 (cell capacitance in peripheral cell model) pF exponentially (see Fig. 6A) and the densities of ionic currents for each cell are functions of its capacitance. In the model, single atrial cells are represented by the Earm-Hilgemann-Noble equations [23]. Electrotonic interactions between cells are modelled by the diffusive interactions of membrane potentials. The equations for the one-dimensional model

$$\frac{dV^{s}(x,t)}{dt} = -\frac{1}{C_{m}^{s}(x)} \left(i_{tot}^{s}(x,t) + D^{s} \frac{dV^{s}(x,t)}{dx} \right)$$
 (1)

$$C_m^s(x) = 20. + \frac{1.07 \times (x - 0.1)}{L^s(1 + 0.7745e^{-(x - 2.05)/(0.295)})} (65 - 20)$$
 (2)

$$\frac{dV^{a}(x,t)}{dt} = -\frac{1}{C_{m}^{a}(x)} \left(i_{tot}^{a}(x,t) + D^{a} \frac{dV^{a}(x,t)}{dx} \right)$$
(3)

$$\left. \frac{dV^s}{dn} \right|_{x=0} = 0 \tag{4}$$

$$\frac{dV^a}{dn} = 0 ag{5}$$

where superscript s denotes SA node, superscript a denotes atrial muscle, C^s_m or $C^a_m(x)$ is the capacitance of a cell x mm distant from the centre of the SA node, Vs or Va(x,t) is its membrane potential, t is the time, Is tot or Ia tot (x,t) is the total current, and Ds or Da is the coupling coefficient which models the electrotonic interactions between SA node cells or atrial cells, respectively. D^s and D^a scale the conduction velocity of the action potential in the SA node and the atrial muscle, respectively. The velocity for near planar waves in the SA node is about 0.001 - 0.1 m/s, and in the atrium about 0.3-0.8 m/s [10]. Efficient numerical solution requires different space steps for SA node and atrial muscle, dx^s and dx^a, respectively. We use non-flux boundary conditions for both ends of the model. Coupling at the junction of the SA node and atrial muscle is by a junctional coupling coefficient D^s. To solve the partial differential equation, we use the explicit Euler method with a 3-node approximation of the Laplacian operator [26]. We fixed dx^sat 0.1 mm, dx^aat 0.3 mm and dt at 0.1 ms. We used $D^a = 1.25$ cm²/s, which gives a conduction velocity of a solitary planar wave of 0.6 m/s in the atrial fiber, and $D^s = 0.6$ cm²/s, which gives a spatial distribution of activation time for cells in the SA node tissue model consistent with the data obtained from the rabbit heart [16].

Figure 5A shows action potentials computed using the one-dimensional model of the intact SA node. Action potentials from various points along the string of cells are shown. The boundary of the SA node and atrium is shown at 0 mm. Figure 5A shows that spontaneous action potentials were first initiated in the centre of the SA node +3 mm from the border of the SA node with the atrial muscle - the action potential then propagated to the periphery of the SA node and then onto the atrial muscle. The activation time is shown in Fig. 6C. This is similar to the activation sequence seen experimentally [16]. The rate of spontaneous action potentials in the one-dimensional model of the intact SA node is 171 beats/min; this is lower than the rate in either the peripheral (384 beats/min) or central (180 beats/min) cell models. However, the rate of spontaneous activity in the one-dimensional model of the intact SA node is comparable to that observed experimentally in the intact SA node of the rabbit, ~170±24 beats/min [25]. The SA conduction time (time for the action potential to conduct out of the SA node) was 45 ms, similar to that seen clinically [1].

Fig. 5B shows how the space constant of the string of rabbit SA node cells was measured - a 2 ms constant current pulse was injected into a SA node cell 2.0 mm from the boundary of the SA node with the atrial muscle. The current was injected during diastole to depolarize the cell at the point of injection by 17 mV. The same technique has been used experimentally [3]. Figure 5B shows that the amplitude of the depolarization declined away from the point of injection. In Fig. 6B, the amplitude of the resulting depolarization is plotted against the distance from the point of injection. The exponential decline in the amplitude of depolarization yields a space constant, 1 of 0.387 mm; this compares to space constants of 0.380 to 0.370 mm measured experimentally in the rabbit SA node [3].

Figure 5A shows that the action potential changes progressively from the atrial muscle to the centre of the SA node. This is confirmed by Fig. 6D, E, F. Figure 6D shows superimposed action potentials at a fast time base at various points along the string of cells; the recordings are comparable to the equivalent experimental recordings [16]. Figure 6E, 6F show various action potential parameters plotted against the distance from the border of the SA node and atrial muscle. The model data are comparable to the experimental data [16].

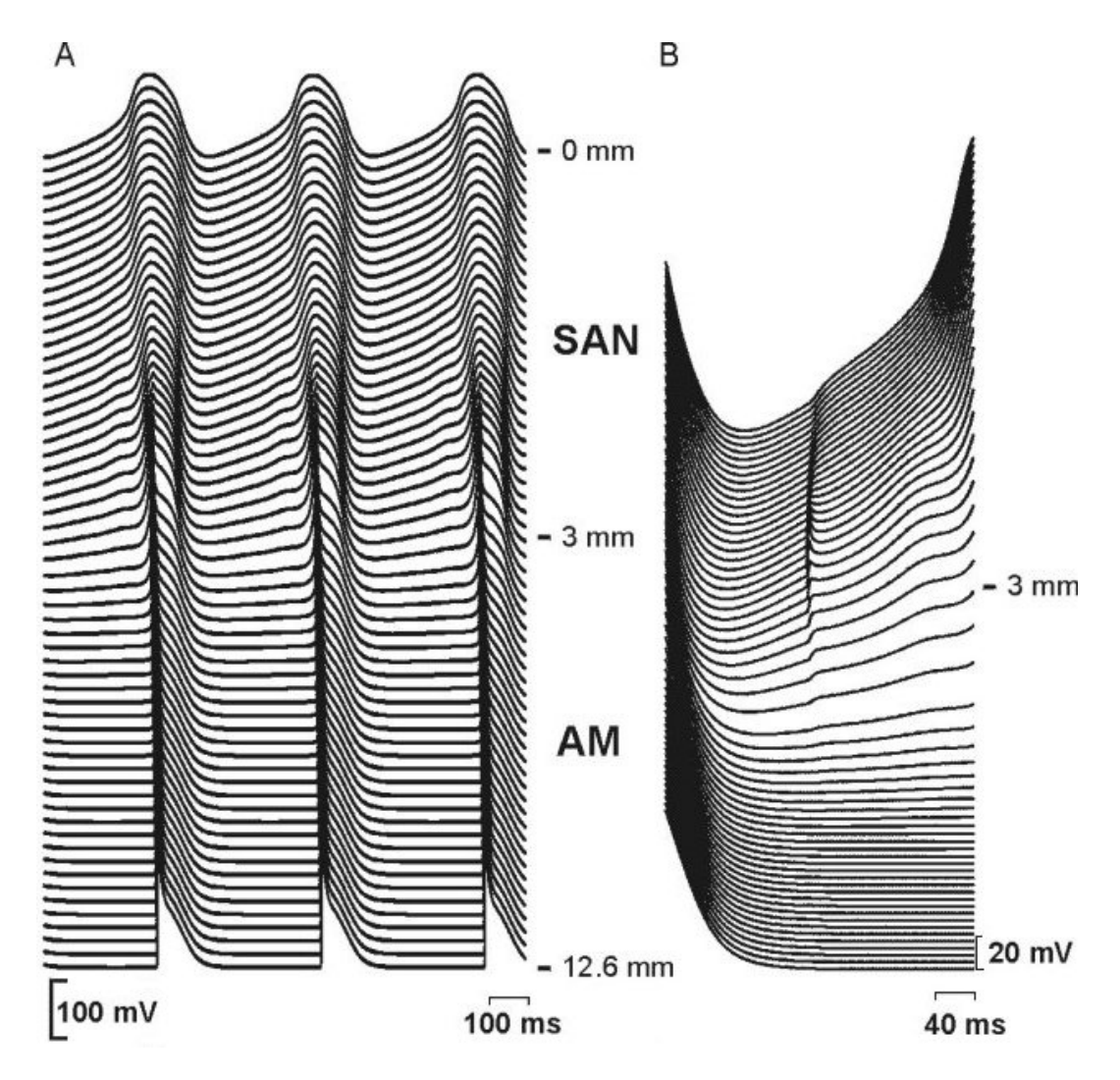


Figure 5. One-dimensional model of the SA node. The propagation of pacemaker activity in the one-dimensional model of sinoatrial node - atrial muscle fibre. A. Computed action potentials are displayed along the length of string of SA node and atrium. 0: mm, the boundary between SA node and atrium; +3.0 mm: the centre of SA node; -9.6 mm, end of atrial string. Action potential is first initiated in the centre of SA node (arrow) and propagates via periphery to atrial muscle. B. Decay of response to 2 ms, 17 mV constant current pulse injected into a SA node cell during diastole 2.0 mm from the boundary of the SA node with the atrial muscle. The amplitude of the depolarization declined away from the point of injection.

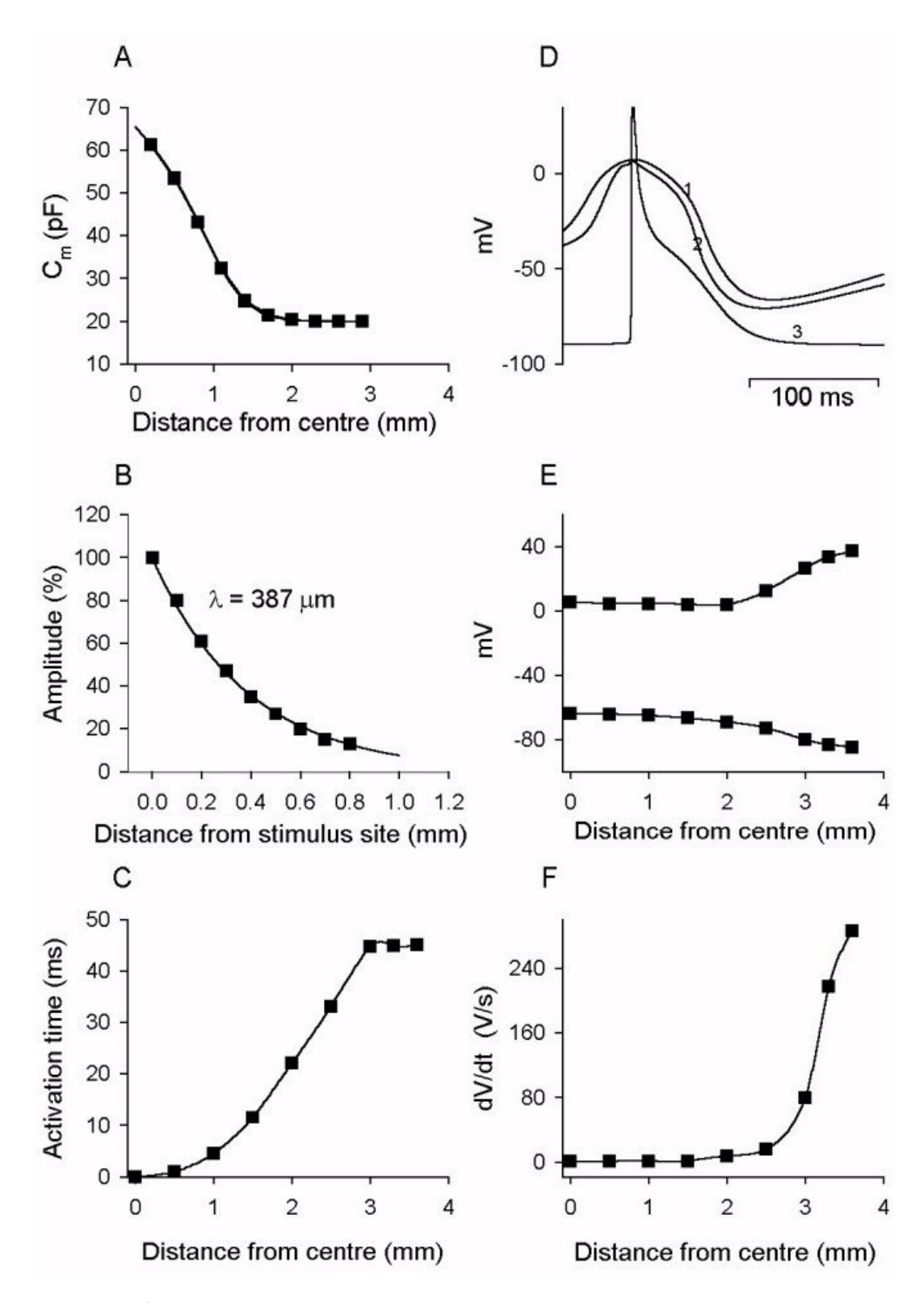


Figure 6. Spatial distributions of characteristics of action potentials along the one-dimensional model. A. spatial distribution of cell membrane capacitance along the SA node fibre. B. spatial distribution of response to a subthreshold stimulus (2 ms in duration) delivered to a point 2mm distance from the border of SA node and atrial muscle during diastolic phase. The decay of the response gives a measure of the space constant of the model. C. spatial distribution of activation time by which the action potential reaches the SA node cells. D. action potentials recorded from cells in different regions in the model fibre. 1: central SA node cell. 2: transitional SA node cell. 3: atrial cell. E. spatial distribution of the overshoot and maximal diastolic potential of action potentials along the fibre. F. spatial distribution of the maximal upstroke velocity of action potentials along the fibre.

Pacemaker shift in mammalian rabbit heart

Figure 7 shows the simulations of the effect of blocking of $i_{Ca,L}$ (simulation of Nifidepine) to the pacemaker activities of the centre SA node. The propagation of pacemaker activities under control condition is shown in panel A. In the control case, the pacemaker activity is initiated at the centre of SA node as pointed by the arrow. In the application of Nifidipine, shown in panel B, which is modelled by blocking i_{CaL} by 50%, the action potential in the centre is abolished, and the leading pacemaker site shifts 2.3 mm towards the periphery of the SA node. This is similar to that observed experimentally [6] and in the model is the result of the presence of TTX-sensitive Na^+ current, i_{Na} , in the periphery, but not the centre, of the SA node: in the periphery, i_{Na} sustains pacemaker activity after partial block of $i_{Ca,L}$.

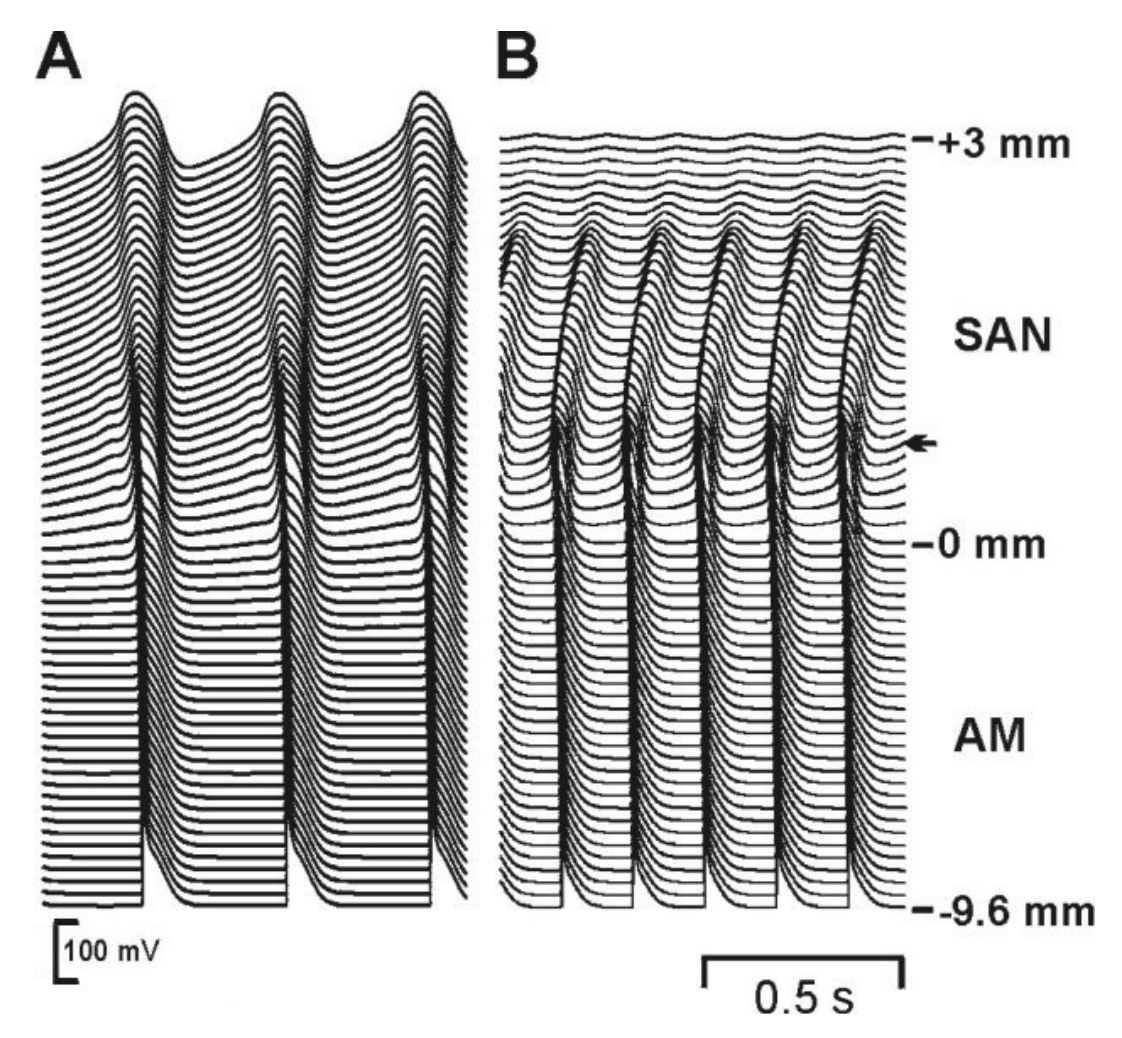


Figure 7. Simulated pacemaker shift by blocking $i_{Ca,L}$. Computed action potentials are displayed along the length of string of SA node and atrium. 0: mm, the boundary between SA node and atrium; +3.0 mm: the centre of SA node; -9.6 mm, end of atrial string. (A) Action potentials under control condition. Action potential is first initiated in the centre of SA node (arrow) and propagates via periphery to atrial muscle. (B) action potentials after 50% block of L-type Ca2+ current. The action potential in the centre is abolished and the leading pacemaker site (arrow) shifts 2.3 mm towards the periphery of SA node.

A hypothesis to explain the conduction block zone:

Mechanism underlying the conduction block zone in SA node is unclear yet. Possible explanations for the block zone are (i) low excitability of cells in the zone and (ii) weak electric coupling between cells in the zone. Experiments have failed to find evidence for weak electric coupling between cells in the block zone [3] and we

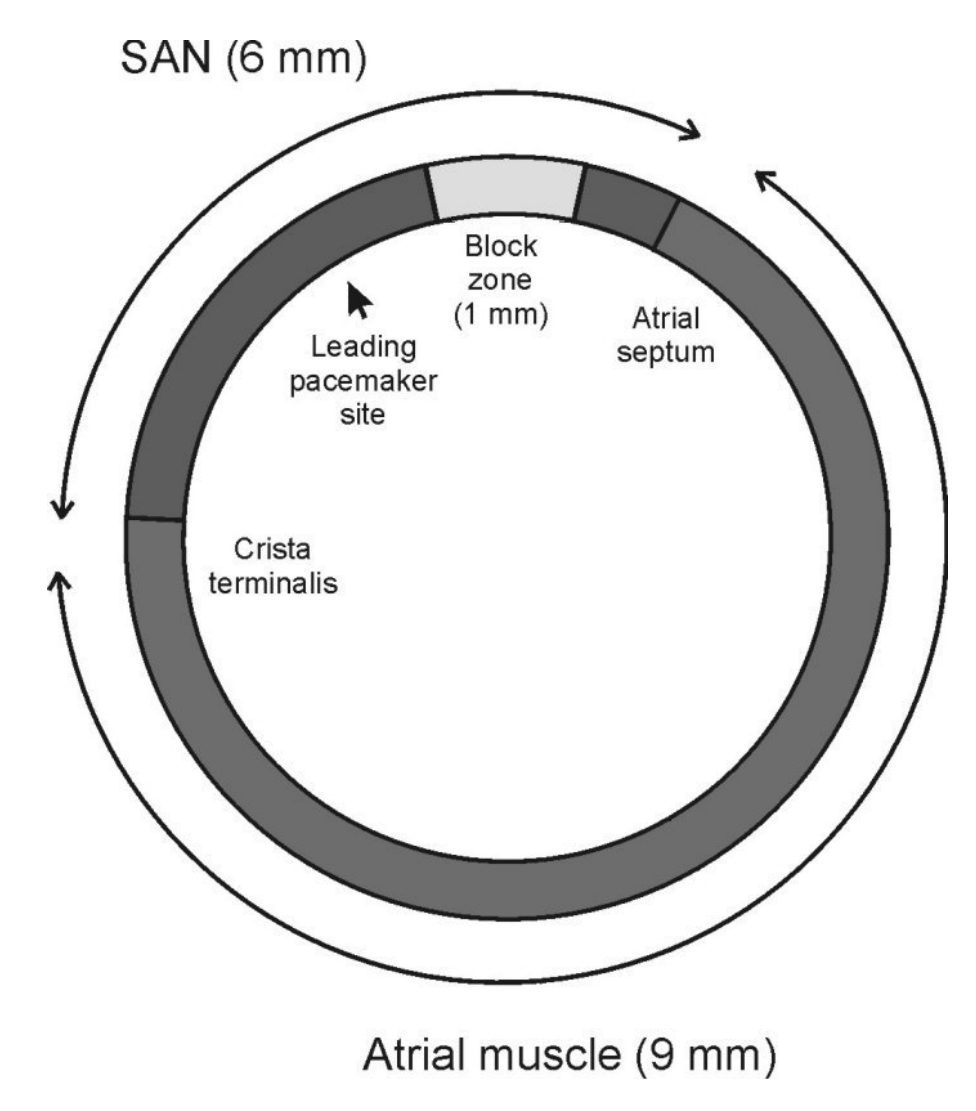


Figure 8. Schematic illustration of a ring model of rabbit sinoatrial node and atrium muscle.

propose that the block zone is the result of low excitability of cells in the zone caused by the absence of the L-type Ca^{2+} current. To test this hypothesis, we constructed a one-dimensional ring model of intact SA node and atrial muscle. The model is schematically illustrated in Figure 8. In the model, the block zone is modelled by removing the L-type Ca^{2+} current, i_{CaL} , from a 1 mm region of the SA node.

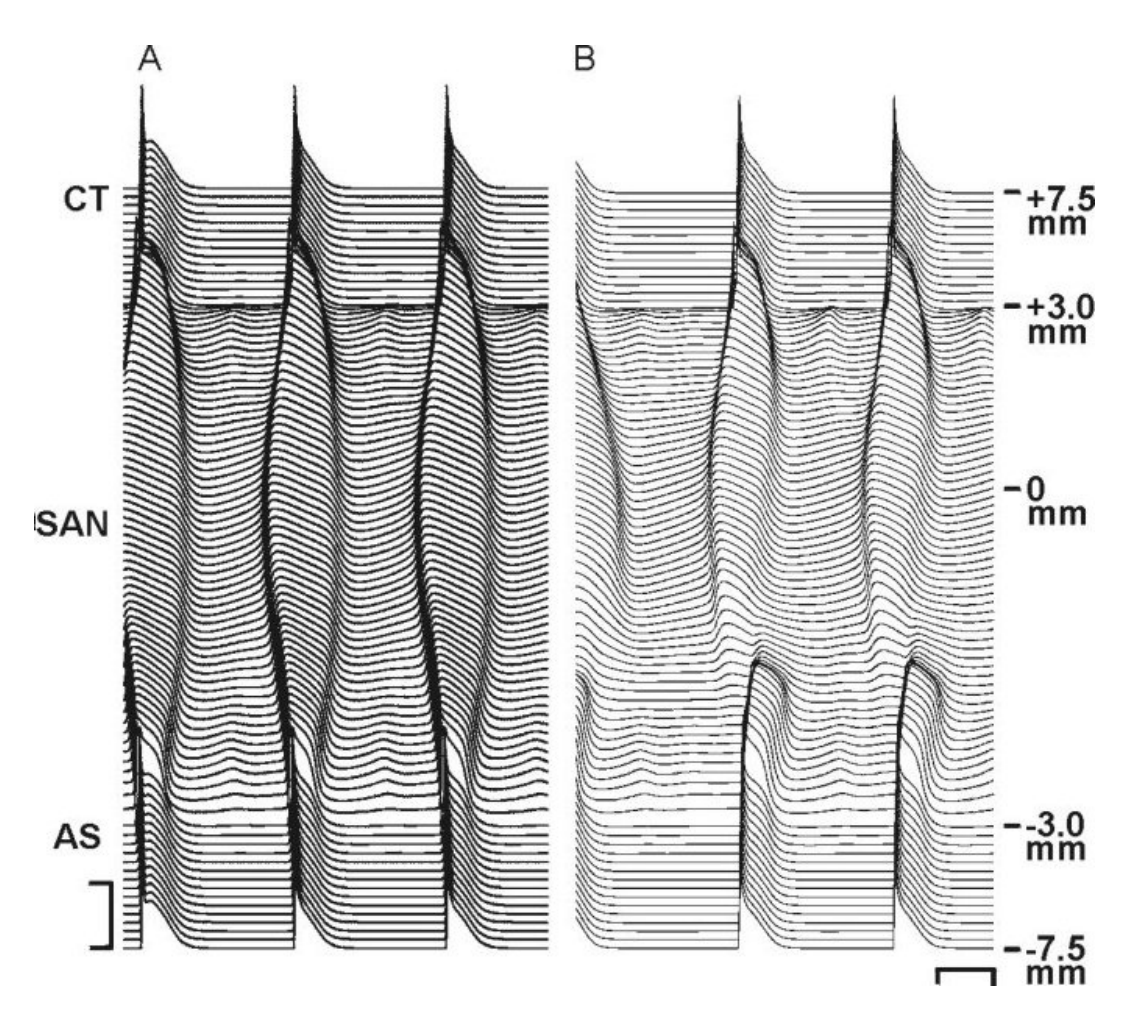


Figure 9. The propagation of action potentials in the one-dimensional ring model of the sinoatrial node and the atrial muscle. A. Symmetric conduction without conduction block zone. The action potential is first initiated in the centre of the sinoatrial node (0 mm), and then propagates towards the periphery (+3 mm) in the direction of CT (+7.5 mm) and towards the periphery (-3 mm) in the direction of AS. B. Asymmetric conduction with a conduction block zone. The action potential is first initiated in the centre of the sinoatrial node (0 mm), and then propagates towards the periphery (+3 mm) in the direction of CT (+7.5 mm). Conduction of action potential towards the periphery (-3 mm) in the direction of CT (-7.5 mm) is blocked due to the block zone caused by removing the L-type Ca^{2+} in the zone. Action potentials conducted from CT to C

Figure 9 shows the propagation of pacemaker activity in the model of a ring of SA node and atrial muscle cells. In the control case, in which there is no conduction block zone, as shown in Fig. 9A, the conduction is symmetric. The pacemaker activity is first initiated in the centre of SA node (0 mm) and then conducts to the periphery of SAN next to the crista terminalis (CT) and the periphery of SAN next to the atrial septum (AS), then onto the atrial muscle. In the test case, as shown in Fig.9B, the conduction is asymmetric. The pacemaker activity is first initiated in the centre of SA node (0 mm) and then conducts to the periphery of SAN next to the crista terminalis (CT) and then onto the atrial muscle of the crista terminalis, conduction of action potentials from the centre of the SA node to the atrial muscle of the atrial septum is activated as a result of the action potential propagating from the crista terminalis around the ring of atrial muscle (equivalent to the situation observed experimentally). The action potential attempts to conduct retrogradely from the atrial septum to the SA node, but it is again blocked in the region lacking the L-type Ca²⁺ current.

Figure 10 shows action potentials recorded from different regions of the model of a ring of SA node and atrial muscle. The AP recorded from the block zone shows a small two-component depolarization. The small two-component depolarization is the result of the collision of action potentials conducted from the centre of the SA node and the atrial septum. Similar small two-component depolarizations are observed in the block zone experimentally [3].

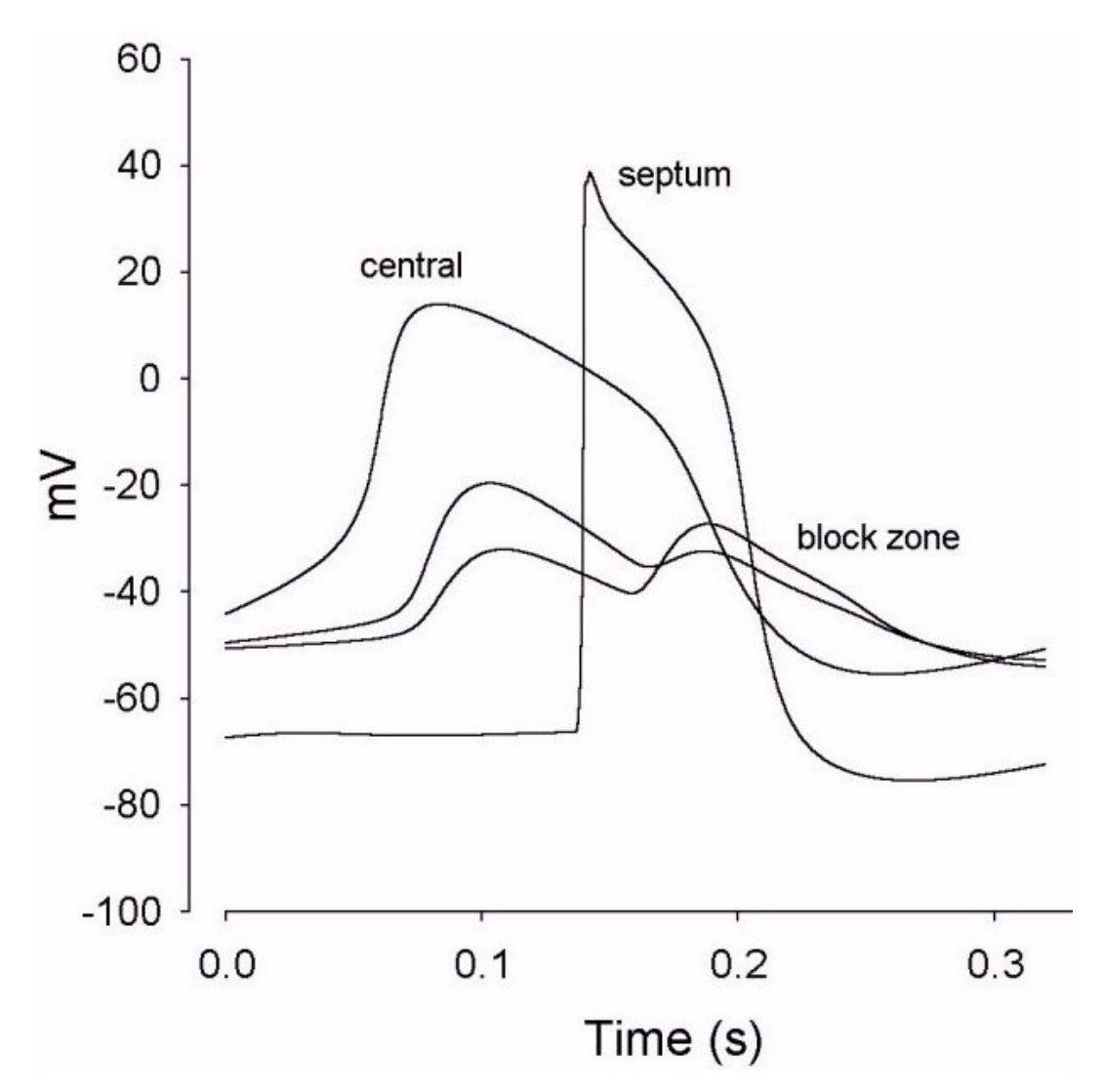


Figure 10. The recorded action potentials from different regions of the one-dimensional ring model of sinoatrial node and the atrial muscle. Action potentials recorded from the block zone show a small two-component of repolarization, which is similar to that seen experimentally.

Biophysically detailed models of electrical activity of central and peripherial sinoatrial node cells are constructed based on the voltage-clamp experimental data from isolated cells of rabbit heart.

Conclusions

The model generated action potentials for the peripheral and central SA node cell are comparable to those recorded from peripheral and central tissue from the rabbit SA node [6,16] as well as those of large and small rabbit SA node cells [12]. Our modelling work *validates* the *assumption* that C_m is an indicator of the region of origin of cells as the models are based on current densities of rabbit SA node cells of different C_m rather than cells isolated from the periphery and centre of the SA node. Experimental work has shown that

block of i_{Na} , 4-AP-sensitive current and i_f has greater effects in peripheral rabbit SA node tissue, whereas block of $i_{Ca,L}$ and $i_{K,r}$ has greater effects in central rabbit SA node tissue [4, 6, 17, 18, 21, 22]. From this indirect evidence, it was argued that the densities of i_{Na} , 4-AP-sensitive current, $i_{K,r}$ and i_f are greater in the periphery than the centre [4, 6, 17, 18, 21, 22]. The modelling was able to support this interpretation, because in the peripheral and central SA node cell models, in which the densities of i_{Na} , 4-AP-sensitive current, $i_{K,r}$ and i_f are greater in the periphery than the centre, the effects of block of these currents as well as $i_{Ca,L}$ are qualitatively similar to those seen experimentally. Block of $i_{Ca,L}$ is a special caseblock of $i_{Ca,L}$ has a greater effect on the centre than on the periphery as a result, in the simulations at least, of the absence of i_{Na} in the centre (in the peripheral model, after block of $i_{Ca,L}$, i_{Na} is able to support the action potential.

Acknowledgements

This work is supported by a programme grant from British Heart Foundation.

References

- [1] Alings, A.M.W. and Bouman, L.N., "Electrophysiology of the ageing rabbit and cat sinoatrial node comparative study", European Heart Journal 14: 1278-1288, 1993.
- [2] Bleeker, W.K., Mackaay, A.J.C., Masson-Pevet, M., Bouman, L.N. and Becker, A.E., "Functional and morphological organization of the rabbit sinus node", Circ.Res. 46: 11-22, 1980.
- [3] Bleeker, W.K., Mackaay, A.J.C., Masson-Pevet, M., Op't Hof, T., Jongsma, H.J. and Bouman, L.N., "Asymmetry of the sino-atrial conduction in the rabbit heart", J. Mol. Cell. Cardiol. 14: 633-643, 1982.
- [4] Boyett, M.R., Honjo, H., Yamamoto, M., Niwa, R. and Kodama, I., "Regional differences in the effects of 4-aminopyridine within the sinoatrial node", Am. J. Physiol. 44: H1158-H1168, 1998.
- [5] Boyett, M.R., Holden, A.V., Kodama, I., Suzuki, R. and Zhang, H., "Atrial modulation of sinoatrial pacemaker rate", Chaos, Soliton& Fractals 5: 425-438, 1995.
- [6] Boyett, M.R., Honjo, H. and Kodama, I., "The sinoatrial node: heterogeneous pacemaker structure" Circulation Res. (in press) 2000.
- [7] Demir, S.S., Clark, J.W., Murphey C.R. and Giles, W.R., "A mathematical model of a rabbit sinoatrial node cell", Am. J. Physiol. 266: C832-C852, 1994.
- [8] Denyer, J.C. and Brown, H.F., "Rabbit sino-atrial node cells: isolation and electrophysiological properties", J. Physiol. 428: 405-424, 1990.
- [9] Dokos, S., Celler, B.G. and Lovell, N.H., "Modification of DiFrancesco-Noble equations to simulate the effects of vagal stimulation on in vivo mammalian sinoatrial node electrical activity", Annals of Biomedical Engineering 21: 321-335, 1999.
- [10] Fozzard, H.A., Haber, E., Jennings, R.B. and Katz, A.M., "The heart and the cardiovascular system", New York: Raven press. 1991.
- [11] Hagiwara, N., Irisawa, H. and Kameyama, M., "Contribution of two types of calcium currents to the pacemaker potentials of rabbit sino-atrial node cells", J. Physiol. 395: 233-253, 1988.
- [12] Honjo, H., Boyett, M.R., Kodama, I. and Toyama, J., "Correlation between electrical activity and the size of rabbit sinoatrial node cells", J. Physiol. 496: 795-808, 1996.
- [13] Honjo, H., Lei, M., Boyett, M.R. and Kodama, I., "Heterogeneity of 4-aminopyridine sensitive current in rabbit sinoatrial node cells", Am. J. Physiol. 276: H1295-H1304, 1999.
- [14] Joyner, R.W. and van Capelle, F.J.L., "Propagation through electrically coupled cells: how a small SA node drives a large atrium", Biophys. J. 50: 1157-1164, 1986.
- [15] Kirchhof, C.J.H.J., Bonke, F.I.M., Allessie, M.A. and Lammers, W.J.E.P., "The influence of the atrial myocardium on impulse formation in the rabbit sinus node", Pflügers Arch. 410: 198-203, 1987.
- [16] Kodama, I. and Boyett, M.R., "Regional differences in the electrical activity of the rabbit sinus node", Pflügers Arch. 404: 214-226, 1985.
- [17] Kodama, I., Boyett, M.R., Nikmaram, M.R., Yamamoto, M., Honjo, H. and Niwa, R., "Regional differences in the effects of E-4031 within the sinoatrial node", Am. J. Physiol. 276: H793-H802, 1999.
- [18] Kodama, I., Nikmaram, M.R., Boyett, M.R., Suzuki, R., Honjo, H. and Owen, J.M., "Regional differences in the role of

- the Ca2+ and Na+ currents in pacemaker activity in the sinoatrial node", Am. J. Physiol. 272: H2793-H2806, 1997.
- [19] Lei, M., Honjo, H. and Boyett, M.R., "Characterisation of the transient outward current in rabbit sinoatrial node cells", In press 2000.
- [20] Masson-Pevet, M.A., Bleeker, W.K., Besselsen, E., Treytel, B.W., Jongsma, H.J. and Bouman, L.N., "Pacemaker cell types in the rabbit sinus node: a correlative ultrastructural and electrophysiological study", J. Mol. Cell. Cardiol. 16: 53-63, 1984.
- [21] Nikmaram, M.R. "Regional differences in the regulation of the rabbit cardiac pacemaker", Ph.D. thesis. University of Leeds. 1996.
- [22] Nikmaram, M.R., Boyett, M.R., Kodama, I., Suzuki, R. and Honjo, H., "Variation in the effects of Cs+, UL-FS 49 and ZD7288 within the sinoatrial node", Am. J. Physiol. 272: H2782-H2792, 1997.
- [23] Noble, D. Oxsoft manual version 4.8. Oxford. 1990.
- [24] Noble, D. and Noble, S.J., "A model of sino-atrial node electrical activity based on a modification of the DiFrancesco-Noble (1984) equations", Proc. R. Soc. Lond.B 222: 295-304, 1984.
- [25] Opthof, T., Van Ginneken, A.C.G., Bouman, L.N. and Jongsma, H.J., "The intrinsic cycle length in small pieces isolated from the rabbit sinoatrial node", J. Mol. Cell. Cardiol. 19: 923-934, 1987.
- [26] Press, W.H., Flannery, B.P., Teukolsky, S.A. and Vetterling, W.T., "Numerical recipies. The art of scientific computing", Cambridge: Cambridge University Press, 1990.
- [27] Schuessler, R.B., Boineau, J.P., and Bromberg, B.I., "", Journal of Cardiovascular Electrophysiology 7, 263-274, 1996.
- [28] ten Velde, I., de Jonge, B., Verheijck, E.E., van Kempen, M.J.A., Analbers, L., Gros, D. and Jongsma, H.J., "Spatial distribution of connexin43, the major cardiac gap junction protein, visualizes the cellular network for impulse propagation from sinoatrial node to atrium" Circ. Res. 76: 802-811, 1995.
- [29] Verheijck, E.E., Wessels, A., van Ginneken, A.C.G., Bourier, J., Markman, M.W.M., Vermeulen, J.L.M., de Bakker, J.M.T., Lamers, W.H., Opthof, T. and Bouman, L.N., "Distribution of atrial and nodal cells within rabbit sinoatrial node. Models of sinoatrial transition", Circulation 97: 1623-1631, 1998.
- [30] Watanabe, Ei-Ichi, Honjo, H., Anno, T., Boyett, M.R., Kodama, I. and Toyama, J. (1996) "Modulation of pacemaker activity of sinoatrial node cells by electrical load imposed by an atrial cell model", Am. J. Physiology 38: H1735-1742.
- [31] Wilders, R., Jongsma, H.J. and van Ginneken, A.C.G., "Pacemaker activity of the rabbit sinoatrial node. A comparism of mathematical models", Biophys. J. 60: 1202-1216, 1991.
- [32] Winslow, R.L., Kimball, A.L., Varghese, A. and Noble, D., "Simulating cardiac sinus and atrial network dynamics on the Connect Machine" Physica D 3: 281-298, 1993.
- [33] Zhang, H., Holden, A.V. and Boyett. M.R., "The pacemaking system of the heart: from coupled oscillators to nonlinear waves", Nonlinear Analysis, Theory, Methods & Applications 30: 1019-1027, 1997.
- [34] Zhang, H., Holden A.V., and Boyett, M.R., "Gradient vs. MOSAIC models of sinoatrial node", Circulation, in press 2000.
- [35] Zhang, H., Holden, A.V., Kodama, I., Honjo, H., Lei, M., Varghese, T. and Boyett, M.R., "Mathematical models of action potentials for centre and periphery sinoatrial node of rabbit heart", Am. J. Physiology (Heart & Circulation), 279 (1): 397-421, 2000.



Official journal of the International Society for Bioelectromagnetism